

Article

A Novel Approach to Enhancing Pesticide Spraying Effectiveness on Citrus Leaves: Adjusting Soil Moisture Content to Improve Leaf Wettability

Xien Zhou ¹, Daozong Sun ², Xiuyun Xue ², Bing Xiahou ³, Qiufang Dai ² and Shuran Song ^{2,4,*}

¹ College of Engineering, South China Agricultural University, Guangzhou 510642, China; season@scau.edu.cn

² College of Electronic Engineering/College of Artificial Intelligence, South China Agricultural University, Guangzhou 510642, China; sundaozong@scau.edu.cn (D.S.); xuexiuyun@scau.edu.cn (X.X.); daiqiufang@scau.edu.cn (Q.D.)

³ General Affairs Department, South China Agricultural University, Guangzhou 510642, China; xiahou@scau.edu.cn

⁴ Key Laboratory of Key Technology on Agricultural Machine and Equipment, Ministry of Education, Guangzhou 510642, China

* Correspondence: songshuran@scau.edu.cn

Abstract: To reduce the amount of pesticides in the environment, it is necessary to consider the wettability properties of pesticide droplets on the leaf surface to improve the spraying effect. The wettability properties of the droplet on the leaf surface are related not only to the properties of the liquid itself but also to the properties of the leaf surface. It is typically believed that leaf surface properties are difficult to control, and thus research has generally ignored this aspect of pesticide use. However, in the field environment, the structure and properties of the leaf surface can be altered by changing the moisture content of the soil where plants are grown. In this study, the roughness, contact angle, and surface free energy of the leaf surface were measured and calculated under different soil moisture contents to study the changes in the leaf surface wettability properties, with the aim of achieving efficient pesticide spraying by adjusting the soil water content. The results showed that the surface composition and microstructure of leaves were altered by the change in the soil moisture content, and the wettability properties of leaves decreased initially and then increased with a decrease in the soil moisture content. When the amount of soil water was sufficient or seriously insufficient, the wettability properties of the leaves were increased, but a lack of soil water may lead to irreversible damage to the plants. Therefore, before spraying pesticides on the leaf surfaces, the plants should be fully watered to improve the wettability properties of the leaf surface, which is conducive to the deposition and adhesion of pesticide droplets on the leaf surface and improved application effectiveness. The results of this study can provide a useful reference for the theoretical research and practices of precision spraying.

Citation: Zhou, X.; Sun, D.; Xue, X.; Xiahou, B.; Dai, Q.; Song, S. A Novel Approach to Enhancing Pesticide Spraying Effectiveness on Citrus Leaves: Adjusting Soil Moisture Content to Improve Leaf Wettability. *Agronomy* **2024**, *14*, 3065. <https://doi.org/10.3390/agronomy14123065>

Academic Editor: Alessandro Suardi

Received: 15 October 2024

Revised: 19 December 2024

Accepted: 20 December 2024

Published: 22 December 2024

Keywords: soil moisture content; droplet; leaf surface; contact angle; wettability



Copyright: © 2024 by the authors. Submitted for possible open access publication under the terms and conditions of the Creative Commons Attribution (CC BY) license (<https://creativecommons.org/licenses/by/4.0/>).

1. Introduction

Spraying pesticides on leaves is one of the most effective ways to prevent and control citrus tree diseases and pests. However, excessive spraying of pesticides and splashing, rebounding, and rolling of droplets in contact with the target during the spraying process not only cause pesticide losses and reduce the efficiency of pesticide use but also pollute the environment [1,2], potentially causing animal poisoning and endangering human health [3]. The research on how to improve the deposition effect of spray droplets on the target is significant for improving the utilization of pesticides [4]. The wettability of pesticide droplets on the leaf surface will directly affect their deposition and adhesion of the

droplets on the leaf surface. Therefore, studying the leaf wettability of droplets on the target leaf surface is important to improve the deposition and adhesion effect of pesticides.

The wettability of the leaf surface is the result of the interaction between the droplet surface tension and the leaf surface properties [3]. The wettability of the leaf surface directly affects the adhesion and spreading properties of pesticide droplets on the leaf [4]. Research has shown that the wettability of the leaf surface is determined by components such as wax on the leaf surface and aspects of the microstructure such as roughness [4–6]. At the same time, the wettability of the droplets on the leaf surface is also affected by the physical and chemical properties of the droplets [1,7]. Therefore, Gao et al. [1] provided a basis for pesticide application by studying the wettability of pear leaves at different stages after flowering in different regions; Kang et al. [8] revealed how the change in leaf structure led to alterations of the wettability by studying the surface morphology and wettability of Katsura leaves from summer to winter; and Jiang et al. [9] studied the microscopic mechanism of leaf wettability through the microstructure and morphology of banana leaves. Leca et al. [10] hypothesized that the wettability could directly express the genetic resistance of apple genotypes, thereby affecting the physicochemical properties of the leaf surface, and revealed that the apple leaf wettability could represent apple scab susceptibility. Papierowska et al. [11] studied the disease resistance of potato varieties by analyzing the relationship between the wettability and leaf trichomes; Zhao et al. [12] and Zhu et al. [13] used ionic surfactants to alter the properties of pesticide droplets to improve the wettability of pesticides on the leaf surface; He et al. [3] proposed methods to improve the wettability by studying the wettability of different test liquids on the surface of rapeseed leaves; and Song et al. [14] investigated the effects of different auxiliaries on the wetting and deposition of insecticide solutions on hydrophobic wheat leaves.

The above research examined the wettability of pesticides by comparing the leaf properties of different plants or by controlling factors other than the plants themselves to seek better spraying parameters and methods to obtain a better deposition effect. In addition to controlling the external factors, changes in the leaf wettability properties also involve plant-related factors, such as alterations in the leaf properties. However, researchers generally assume that the plant leaf properties are difficult to control, and thus there are few studies in this area. However, the surface properties of leaves are easily affected by external environmental factors such as temperature, humidity, and sunlight intensity. For field planting, these factors are difficult to control, but the soil moisture content is relatively easy to control, and the soil moisture content can significantly affect the leaf properties. Changes in the soil moisture content affect the wettability of leaves by affecting the changes in leaf surface properties such as leaf surface structure or chemical composition, which in turn can affect the deposition of droplets. Therefore, it is of both theoretical and practical significance to study the effect of the soil moisture content on the wettability properties of droplets on citrus leaves.

The commonly used wettability quantification parameters include the contact angle and surface free energy [15,16]. The contact angle is defined as the angle formed by the intersection of the liquid–solid interface and liquid–vapor interface; this can quantify the wettability of a solid surface [17–19]. The size of the contact angle will be affected by the properties of the test liquid and the properties of the solid surface. It is generally believed that a contact angle between the droplet and the solid surface greater than 90° indicates that the surface is hydrophobic and difficult to wet. A contact angle of less than 90° indicates that the surface is hydrophilic and can be easily wetted by liquids [3,20]. The free surface energy is an inherent property of the solid surface and does not change with the test liquid [21]. The surface free energy and its components are one of the basic thermodynamic properties of solid surfaces and are also important parameters for measuring the surface wettability. The surface free energy is calculated by measuring the contact angle of different detection liquids on a solid surface using certain methods [22]. In general, the greater the surface free energy, the better the wettability of the leaf [7,23].

Therefore, by controlling the water content of the soil where the plant grows, this study examined the variation in leaf surface roughness, contact angle, and surface free energy under different soil water contents, aiming to achieve efficient pesticide spraying by adjusting the soil water content. The results can provide a useful reference for the theoretical research on precision pesticide application and the practice of field application.

2. Materials and Methods

2.1. Plant

The test plant was a 3-year-old *Citrus reticulata* 'Sha tangju' seedling (a *Rutaceae citrus* species grafted with *Poncirus trifoliata* as the rootstock). After the plant had grown in the orchard for three years, it was transplanted into a pot. The experiment was carried out after the fruit tree had produced new leaves. To reduce the influence of changes in the leaf structure caused by leaf growth during the test, mature and unshielded leaves were used for the experiment.

2.2. Test Environment

To avoid the influence of other environmental factors, the plant was placed in the plant environment conditioning room three days before the experiment. The humidity of the conditioning room was $70 \pm 6\%$, and the temperature was $24 \text{ }^\circ\text{C} \pm 0.5 \text{ }^\circ\text{C}$. The plant was placed under a full-spectrum plant growth lamp (100wUFO, YIRUNFA, Shantou, China). The growth lamp was turned on from 6:00 to 19:00 every day. The leaves used in the experiment were in the light intensity range of 20,000–23,000 lux, and the relative position between the experimental leaves and the plant growth lamp remained unchanged throughout the experiment.

2.3. Methods

2.3.1. Soil Moisture Content Setting

The target soil moisture content was obtained via natural absorption and evaporation. Before the test, the soil was fully irrigated, and the soil moisture content was measured at 7 a.m. every day. The experiment was conducted using the soil moisture contents of $80.5 \pm 1\%$, $68.8 \pm 1.2\%$, $56.9 \pm 0.9\%$, $45.8 \pm 2.7\%$, and $35.6 \pm 0.6\%$ of the field water capacity. The five soil moisture contents were labeled as T5, T4, T3, T2, and T1, respectively. The field water capacity, measured using the method of Gao et al. [24], was determined to be 29.5%.

2.3.2. Leaf Selection and Treatment

Dust and other impurities on the leaf surface will have a significant impact on the experimental data. Therefore, while fully watering the plant, clean water was sprayed on the experimental leaves through a small hand-held sprayer, and the adaxial and abaxial surfaces of the leaves were washed several times. During the spraying process, the leaf surface was not touched with hands or wiping tools to avoid damaging the leaf structure and thereby affecting the accuracy of the test. The test leaves were marked.

Starting from the soil moisture content T5, the experiment was carried out sequentially from T5 to T1 as each target moisture content was reached, and two groups of experiments were carried out each time. The experiments comprised measuring the contact angle and roughness of the adaxial and abaxial surfaces of the leaf. Since the surface structure of different leaves may vary, each experiment of the same group under different soil moisture contents was carried out on the same leaf. Due to the limited available leaf area, different groups of experiments were carried out on different leaves. Figure 1 shows the leaf areas used for each test. Each experiment was carried out after cutting off the experimental area of the leaf using scissors. To avoid the previous cut edge influencing the results of the subsequent leaf surface measurement, a sufficient distance was maintained from the previous cut edge during each subsequent cut. To keep the surface structure and

composition of the detached leaf essentially unchanged, the test was performed immediately after the leaf was cut off, and the data collection was completed within 15 min. When picking leaves, we used tweezers to clamp the edges of the cut leaf area; these were fixed to glass slides using double-sided adhesive tape and used for testing after gentle compacting [25]. Thicker leaf veins were avoided.

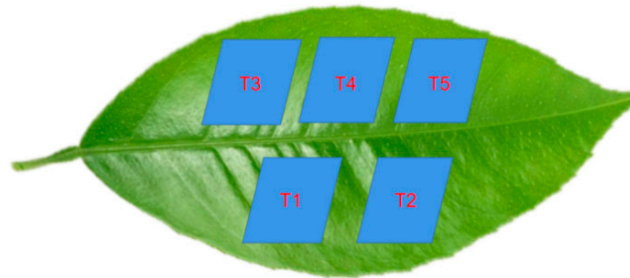


Figure 1. Division of the leaf test area.

2.3.3. Leaf Surface Feature and the Roughness Factor

There are many accurate methods for leaf surface feature observation and roughness measurement, including observing the blade surface structure using a scanning electron microscope and the measuring blade surface roughness using an atomic force microscope. However, due to the high real-time requirements of this test, the super depth of field 3D microscope (vhx-900f, KEYENCE, Osaka, Japan) was used to directly observe the surface features of the adaxial and abaxial surfaces of the leaves. This method retains the original shape of the leaf surface and can obtain a three-dimensional microstructure of the sample close to its physiological state, and the method can nondestructively measure the leaf surface feature parameters, as shown in Figure 2.

When observing the structural features of the leaf surface, the microscope magnification was set to 1000 \times , and clear images were obtained by taking photos. The super depth of field 3D microscope used in the experiment cannot directly measure surface roughness, but it can measure the surface area of the relevant region and the corresponding projected area (the measurement accuracy is 0.1 μm^2) through its fast synthetic SD image function of “depth UP.” The roughness factor R is the ratio of the surface area to the projected area. For the 3D image acquisition, the microscope magnification was 500 \times , and more than seven valid data points were collected in each experimental area to calculate the roughness factor. The average value of the roughness factor in each experimental area is obtained from both the roughness factor of the adaxial and abaxial surfaces of the leaf.

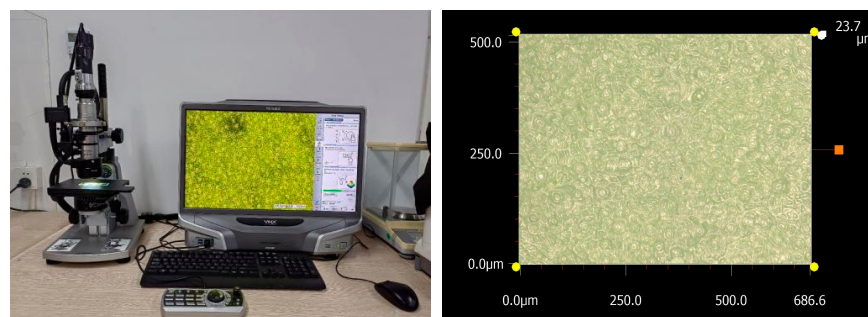


Figure 2. Observation and measurement of leaf surface structure. The yellow dots are used to measure the area, the white dot represents the highest point, and the orange dot is used to adjust the display angle.

2.3.4. Static Contact Angle Measurement and the Contact Angle Model

The contact angle of the test liquids on the adaxial and abaxial surfaces of the leaf was measured using a contact angle measuring instrument (capst-2000at, PST, Dongguan, China), as shown in Figure 3. Distilled water and N, N-dimethylformamide were used as the test liquids, and the seat drop method was used for measurement. A 2 μL droplet was generated using a micro syringe (with a range of 1000 μL and accuracy of 0.1 μL) included in the instrument, and then the stage on which the glass slide was placed was adjusted to make the droplet make contact with the leaf surface. The stage was readjusted to make the droplet leave the micro syringe needle. After 35 s, when the droplet was stable, the static contact angle was measured by using the instrument's software (ContactAnglemeter 2.0).

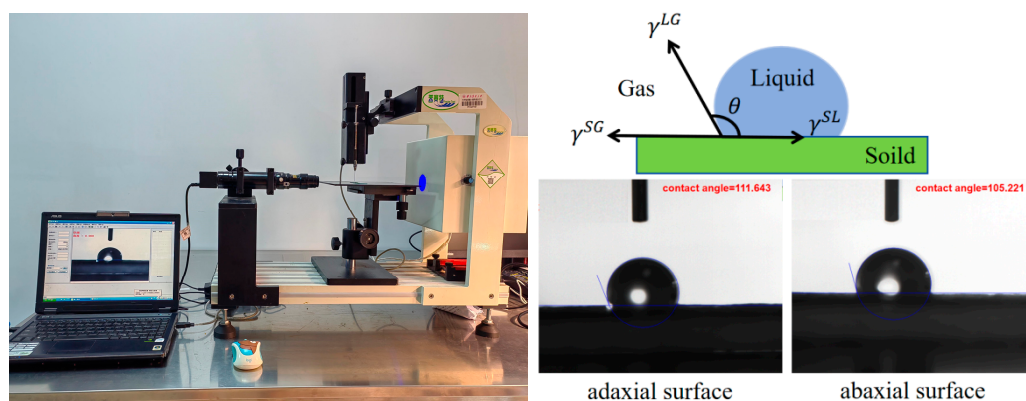


Figure 3. Static contact angle measurement, where θ is the contact angle.

The contact angle is the angle formed at the junction of the solid, liquid, and gas phases, and it can be used to quantify the degree of wetting of the solid surface. Depending on whether the contact interface is smooth and the interaction between the droplet and the rough solid surface, the contact angle can be described using the Young model [26], Wenzel model [27], Cassie model [28], or Cassie–Baxter model [29], as shown in Figure 4.

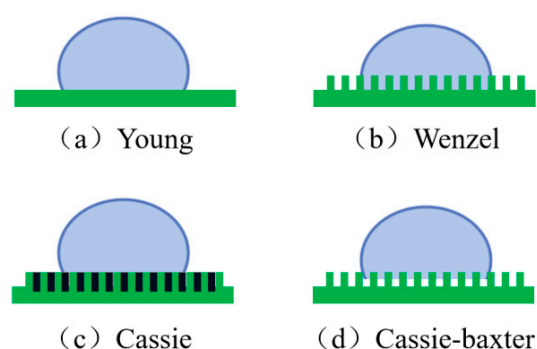


Figure 4. Contact angle model.

The Young model is an idealized model; it assumes that the solid surface is smooth, rigid, chemically homogeneous, and has no chemical reaction, and that the line tension at the three-phase contact line is negligible. However, in practical applications, most solid surfaces have a degree of roughness. The Wenzel model assumes that the solid surface is a rough surface with many grooves, allowing the liquid to completely infiltrate into these grooves upon contact with the solid surface. A simple equation is used to describe the contact angle model of the rough surface, and is shown in Equation (1). The Cassie model assumes that the solid surface is composed of a rough surface of heterogeneous composite

materials, and its calculation formula is shown in Equation (2). In cases when one of the materials in the Cassie model is air—that is, when droplets cannot fully infiltrate the solid grooves—air is left in the rough surface groove. At this point, the contact surface consists of two parts: the interaction between the droplet and the elevated solid surface and the interaction between the droplet and the air. This transformation from the Cassie model to the Cassie–Baxter model is expressed by its calculation formula, which is shown in Equation (3).

$$\cos \theta_a = R \cos \theta_e \quad (1)$$

$$\cos \theta'_a = \sigma_1 \cos \theta_{e1} + \sigma_2 \cos \theta_{e2} \quad (2)$$

$$\cos \theta_a = \sigma_1 \cos \theta_{e1} - \sigma_2 \quad (3)$$

where R is the roughness factor of the solid surface; $R \geq 1$; θ_a is the measured contact angle, also known as the apparent contact angle; θ_e is the contact angle of the smooth surface, also known as the intrinsic contact angle; θ'_a is the apparent contact angle of the composite material; σ_1 and σ_2 are the area fractions of the two contact surfaces, respectively; θ_{e1} and θ_{e2} are the intrinsic contact angles of material 1 and material 2, respectively.

From the above contact angle models, it can be seen that changes in the solid surface structure can lead to differences in the contact angle model, thus changing its wettability.

2.3.5. Calculation of the Apparent Surface Free Energy

The surface free energy of the leaf surface was calculated by reference to the static contact angle of different test liquids on the leaf surface. Since the measured contact angle is affected by the chemical composition and microstructure of the leaf surface, the calculated leaf surface free energy is also known as the apparent surface free energy [30]. There are many methods for calculating the apparent surface free energy [30], including the “one liquid method,” where it is necessary to measure the contact angle of a detection liquid on the solid surface, including methods such as ZDY and Neumann; the “two liquids methods,” such as OWRK and HM; and “three liquids methods,” such as OCG.

In this study, the OWRK method [23,25,31] was used to calculate the apparent surface free energy and its components for the adaxial and abaxial surfaces of the blade. The OWRK method is expressed as follows:

$$\gamma_{sl} = \gamma_l + \gamma_s - 2 \left(\gamma_l^d \gamma_s^d \right)^{\frac{1}{2}} - 2 \left(\gamma_l^p \gamma_s^p \right)^{\frac{1}{2}} \quad (4)$$

where γ_{sl} , γ_l , and γ_s are the interfacial free energies between a solid and liquid, the surface free energy of a liquid in equilibrium with the saturated vapor of the liquid, and the surface free energy of the solid, respectively; γ_l^d and γ_s^d are the nonpolar components (dispersion components) of the surface free energy of a solid and liquid, respectively, and γ_l^p and γ_s^p are the polar components of the surface free energy of a solid and liquid, respectively.

Through Equation (5), Young’s equation represents the relationship between the contact angle θ of liquid droplet formation on a solid surface and the three interface free energies of solid, liquid, and gas:

$$\cos \theta = (\gamma_s - \gamma_{sl}) / \gamma_l \quad (5)$$

Combining Equations (4) and (5), we obtain Equation (6):

$$\gamma_l (1 + \cos \theta) = 2(\gamma_l^d \gamma_s^d)^{\frac{1}{2}} + 2(\gamma_l^p \gamma_s^p)^{\frac{1}{2}} \quad (6)$$

According to Equation (6), the polar component γ_s^p and non-polar component γ_s^d of a solid surface can be calculated by measuring the contact angles of the two test liquids with a known surface free energy γ_l and its polar component γ_l^p and non-polar component γ_l^d on the solid surface, and then the corresponding surface free energy of the solid can be obtained via Equation (7):

$$\gamma_s = \gamma_s^p + \gamma_s^d \quad (7)$$

3. Results

3.1. Leaf Surface Features

Figure 5 shows the surface features of the adaxial and abaxial surfaces of the leaves used in the test. The figure shows that there is no fluff on the adaxial or abaxial surfaces of the blade, but the surface is rough and full of folds. There are no stomata on the adaxial surface of the leaf, while the abaxial surface is full of stomata, and the distribution is uniform. There were no significant differences observed in the leaf surface features obtained using the super depth of field 3D microscope under different soil moisture treatments.

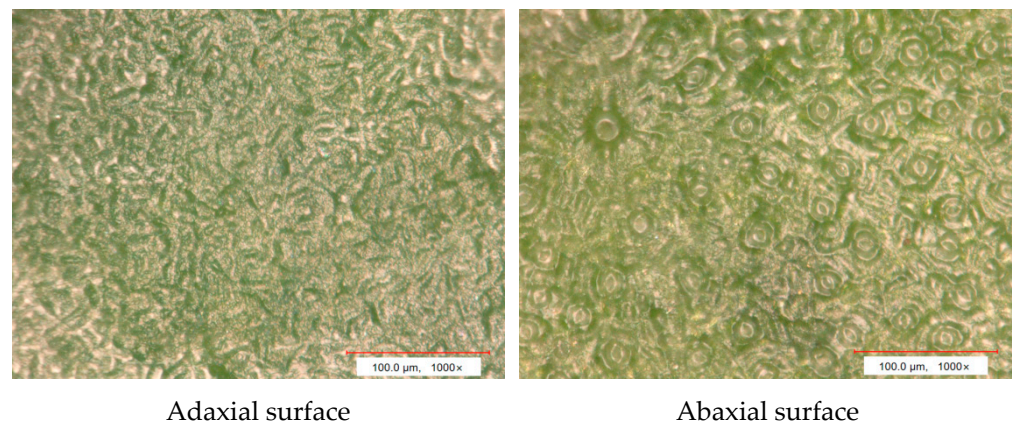


Figure 5. Leaf surface features.

3.2. Leaf Surface Roughness Factor

Figure 6 shows the relationship between the leaf adaxial and abaxial roughness factors and the soil moisture content. As shown in the figure, there was no significant difference in the observed surface roughness factor with a decrease in the soil moisture content in both the adaxial and abaxial leaf surfaces. However, the abaxial surface roughness factors were significantly higher than those of the adaxial surface under the same soil moisture content.

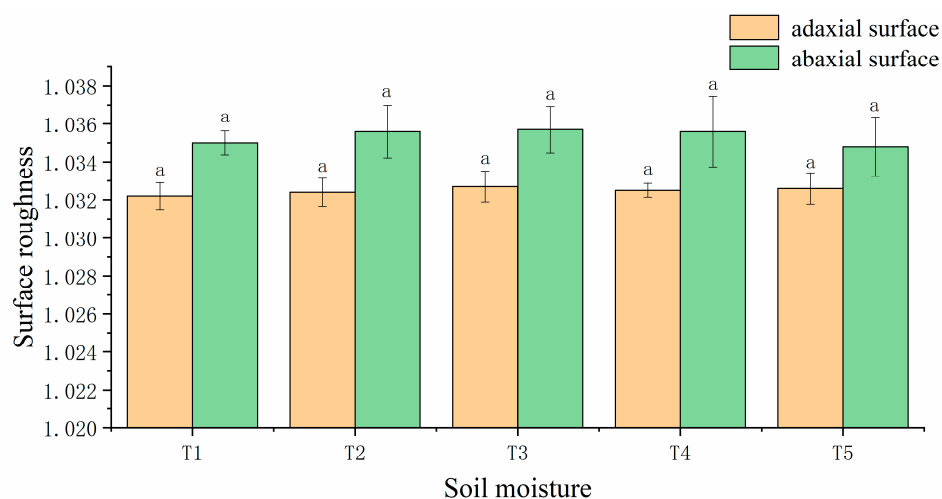


Figure 6. Roughness factors of adaxial and abaxial surfaces of leaves. Different lowercase letters indicate significant differences ($p < 0.05$), while the same lowercase letters indicate non-significant differences, as calculated using ANOVA followed by Tukey's test.

3.3. Static Contact Angle and the Apparent Surface Free Energy of Leaves

Figure 7 shows the variation in the static contact angle of distilled water on the leaf surface at the different soil moisture contents. The static contact angles of the adaxial and abaxial surfaces of the leaf were both greater than 90, showing hydrophobicity. The static contact angles of the adaxial and abaxial surfaces increased initially and then decreased with the decrease in the soil moisture content. Except for the case where the static contact angle of the adaxial surface of the leaf is smaller than that of the abaxial surface at T5, the static contact angle of the adaxial surface was greater than that of the abaxial surface under the other values of the soil moisture content.

Figure 8 shows the variation in the static contact angle of the N, N-dimethylformamide test liquid on the leaf surface under the different values of the soil moisture content. The static contact angles of the adaxial surface and the abaxial surface of the leaf were both less than 60, which was lower than that of distilled water on the leaf surface. When the soil moisture content was low, there was no significant difference in the static contact angle between the adaxial surface and the adaxial surface of the leaf, but a noticeable difference appeared when the soil moisture content was high.

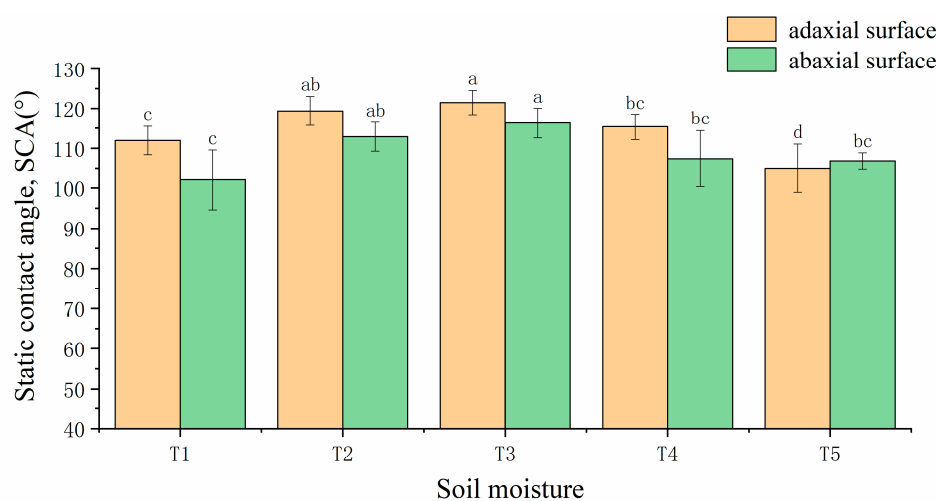


Figure 7. Static contact angle of distilled water on the leaf surface. Different lowercase letters indicate significant differences ($p < 0.05$), while the same lowercase letters indicate non-significant differences, as calculated using ANOVA followed by Tukey's test.

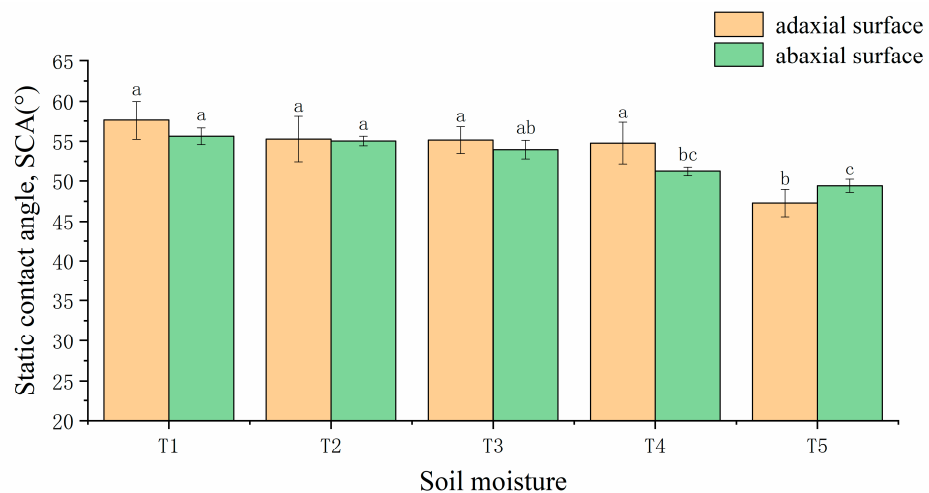


Figure 8. Static contact angle of N, N-dimethylformamide on leaf surface. Different lowercase letters indicate significant differences ($p < 0.05$), while the same lowercase letters indicate non-significant differences, as calculated using ANOVA followed by Tukey's test.

The apparent surface free energy and its components of distilled water and N, N-dimethylformamide are shown in Table 1 [25].

Table 1. Apparent surface free energy and its components of test liquids.

Test Liquid	Apparent Surface Free Energy (mJ/m^2)	Dispersion Component (mJ/m^2)	Polar Component (mJ/m^2)
Distilled water	72.8	29.1	43.7
N, N-dimethylformamide	37.3	32.42	4.88

Using the static contact angles of distilled water and N, N-dimethylformamide on the leaf adaxial and abaxial surfaces, the apparent surface free energy and its components were calculated by using the OWRK method, as shown in Table 2.

Table 2. Apparent surface free energy and its components on the adaxial and abaxial surfaces of the leaf.

Leaf Surface	Polar Component	T5 (mJ/m^2)	T4 (mJ/m^2)	T3 (mJ/m^2)	T2 (mJ/m^2)	T1 (mJ/m^2)
Adaxial surface	Apparent surface free energy	18.61	6.23	5.44	5.03	10.24
	Polar component	0.35	2.43	5.27	4.13	0.92
	Dispersion component	18.26	3.80	0.17	0.90	9.32
Abaxial surface	Apparent surface free energy	15.64	15.42	5.68	8.39	25.35
	Polar component	0.54	0.50	2.98	1.51	0.06
	dispersion component	15.10	14.92	2.70	6.88	25.28

It can be seen from Table 2 that the apparent surface free energy of the adaxial and abaxial surfaces was low and basically showed a trend of first decreasing and then increasing with the decrease in the soil moisture content. On the adaxial surface, the leaf had the maximum apparent surface free energy at T5, and the apparent surface free energy values at T2, T3, and T4 were much less than $10 \text{ mJ}/\text{m}^2$. However, on the abaxial

surface, only T2 and T3 had an apparent surface free energy less than 10 mJ/m², with the maximum surface free energy exceeding 20 mJ/m² at T1. At T5, the apparent surface free energy of the adaxial surface was slightly greater than that of the abaxial surface. The surface free energy of the abaxial surface was greater than that of the adaxial surface under the other values of the soil moisture content. The reason for this is that the maximum and minimum values of the apparent surface free energy of the adaxial and abaxial surfaces appeared at the different soil moisture contents, which may be caused by the differences in their surface structures. In particular, the abaxial surface is affected by the opening and closing of the stomata, and the apparent surface free energy changes more significantly.

Figure 9 shows that as the soil moisture content decreased, the proportion of dispersion components on the adaxial and abaxial surfaces decreased initially and then increased, while the polar components increased initially and then decreased. On the adaxial surface, the dominance of the apparent surface free energy component also changes accordingly, with the dispersion component dominating at T5, T4, and T1, and the polar component dominating at T3 and T2. The change in the dominance of the apparent surface free energy component on the abaxial surface was also similar to that on the adaxial surface, but only at T3 did the polar component dominate, and it exhibited minimal differences from the dispersion component. The dispersion component of the abaxial surface was somewhat more dominant than that of the adaxial surface, consistent with its higher apparent surface free energy.

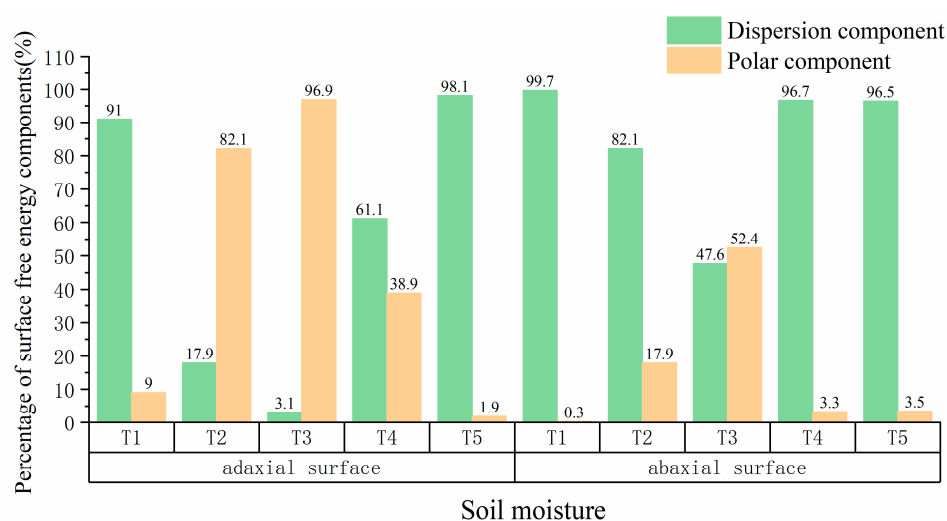


Figure 9. Proportion of apparent surface free energy components.

4. Discussion

4.1. Effect of the Soil Moisture Content on the Leaf Surface Features

Studies have shown that the surface roughness is affected by the microstructure of the leaf surface [32]. The roughness is an important factor affecting the dynamic wetting behavior of the leaf surface [33].

Figure 6 shows that the leaf surface structure changed little under the different soil moisture conditions as observed by using the super depth of field 3D microscope. Therefore, although there were some differences in the same leaf surface roughness factors under the different values of the soil moisture content, the differences were not significant. The significant difference in the roughness factor between the abaxial surface and the adaxial surface was primarily due to the difference in the surface microstructure. In addition to the folds, the abaxial surface of the leaf is also full of stomata, making the abaxial surface of the leaf more rough.

4.2. Effect of the Soil Moisture Content on the Leaf Wettability

The wettability of the leaf surface is not only affected by the properties of the pesticide solution itself but is also affected by the leaf surface properties [25]. The leaf surface properties include the leaf surface composition and microstructure such as the waxy chemical composition of the leaf surface layer, the surface topology, and roughness [33]. Although the difference in leaf structure and roughness was not apparent when the leaf surface structure was observed and measured by using the super depth of the field 3D microscope, a slight change in its microstructure or leaf surface composition may be sufficient to affect the wettability of the leaf surface.

On rough surfaces, the contact angle models are generally classified into three types: the Wenzel model, the Cassie model, and the Cassie–Baxter model, as shown in Figure 4. We assumed that the contact angle model followed the Wenzel model. On rough surfaces, droplets can penetrate completely into the grooves on solid surfaces. The apparent contact angle can be expressed by the Wenzel equation, as shown in Equation (1). When the intrinsic contact angle θ_e and roughness factor R of the leaf surface remain unchanged, the apparent contact angle of the leaf surface should also remain unchanged. However, from Figures 6 and 7, it can be seen that the roughness factor is not significantly different under the different soil moisture contents. In contrast, the contact angle between the adaxial and abaxial surfaces is significantly different, first increasing and then decreasing with a decrease in the soil water content. Therefore, the assumption that the contact angle model follows the Wenzel model under each soil moisture content contradicts the experimental results. This indicates that with the change in the soil moisture content, the composition and structure of the leaf surface were altered, thereby resulting in a change in the intrinsic contact angle and causing there to be differences in the contact angle model throughout the experiment. A significant alteration of the dispersion component and the polar component of the apparent free energy as shown in Figure 9 also indicated that the leaf surface has been altered.

Therefore, the change in the contact angle may be due to slight changes in the composition and microstructure of the blade surface, resulting in a change in the wetting state of the blade surface [30], as shown in Figure 10. When the soil moisture content is high, the wetting state of the leaves follows the Wenzel or Cassie–Baxter model. As the soil moisture content decreases, the leaf surface components or microstructure changes, and the leaf wetting status changes from Wenzel (or Cassie–Baxter) to Cassie–Baxter (or Cassie–Baxter) before transitioning to Wenzel (or Cassie–Baxter) status. Thus, the contact angle increases initially and then decreases with the decrease in the soil moisture content. Further in-depth research is needed on how to transform the composition of the leaf surface.

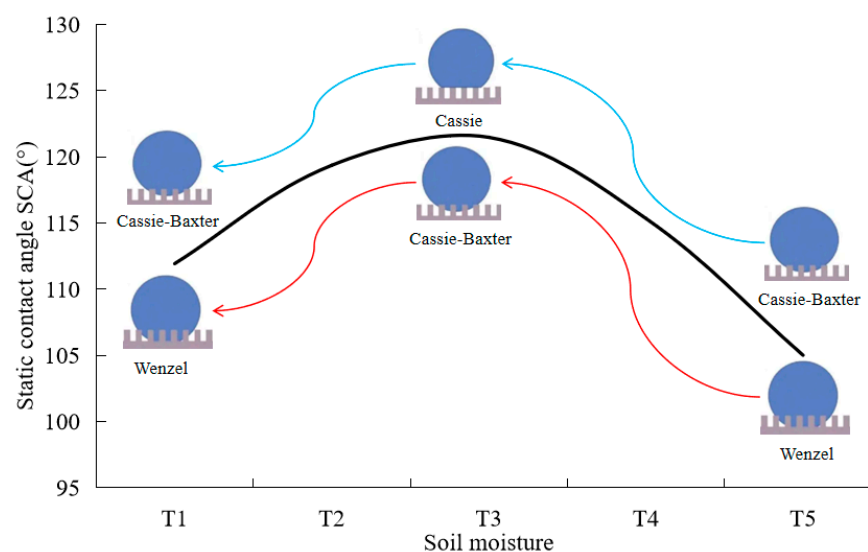


Figure 10. Transition of wetting state. The red and blue lines represent two wetting status transitions that can occur.

A surface free energy of 0–20 mJ/m² indicates a highly hydrophobic state; 20–40 mJ/m² indicates a hydrophobic state; and above 40 mJ/m² indicates a hydrophilic state [1]. The apparent surface free energy of the leaf used in this experiment was 5.03–25.35 mJ/m², indicating a low-energy surface and a hydrophobic to highly hydrophobic state. When the surface free energy (surface tension) of the droplet onto the solid surface is less than the surface free energy of the solid, the liquid can wet the solid surface. The closer the surface free energy of a liquid is to that of a solid, the easier it is to spread the liquid over the solid surface [34]. Therefore, under all the soil moisture conditions, the apparent surface free energy of N, N-dimethylformamide was closer to the apparent surface free energy of leaves than distilled water. The contact angle was much smaller than that for distilled water, and it was easier for droplets to spread on the leaf surface.

According to Table 2 and Figure 9, the change rule of the leaf apparent surface free energy was consistent with the change rule of the dispersion component, showing that with the decrease in the soil moisture content, the surface free energy decreases initially and then increases.

It is generally believed that when the dispersion component of the apparent surface free energy is dominant, a solid surface is hydrophobic, while when the polar component is dominant, a solid surface is hydrophilic [7]. However, according to our experimental results, with the change in the soil moisture content, the dominance of the dispersion component and polar component of the apparent surface free energy was altered. For the adaxial surface at T2 and T3 and the abaxial surface at T3, the polar component was dominant, but the solid surface was not hydrophilic, similar to some experimental results obtained previously [1,34]. This may be due to the different composition of the leaf surface.

According to the changes in the static contact angle and the apparent surface free energy of the leaf surface, the wettability of the leaf surface first decreases and then increases with the decrease in the soil moisture content, and the wettability is better when the soil water content is sufficient or when there is a severe water shortage.

5. Conclusions

This study aims to investigate how the variations in the soil moisture content affect the microstructure and composition of leaves and to examine further how these changes affect the leaf wettability. Our main findings indicate that as the soil moisture content decreases, the wettability of leaves initially declines and then subsequently increases. Maintaining the soil moisture either in an adequate state or a severely insufficient state

can enhance the leaf wettability; however, extreme water scarcity may cause irreversible damage to plants. Therefore, to achieve the optimal leaf wettability and improve the effectiveness of foliar applications, it is recommended that plants are thoroughly watered before the application of pesticides. This research underscores the significant influence of the soil moisture content as the sole adjustable environmental factor in field conditions on the leaf wettability. The results of this study provide an important contribution to the understanding of droplet deposition enhancement, thereby advancing the development of precision spraying techniques in agriculture.

Nonetheless, the limitations of this study include its focus on specific plant varieties, which may restrict the generalizability of the findings. Additionally, while the study explored the effects of the soil moisture on the wettability, the interactions with other environmental factors have not been sufficiently investigated. Future research directions should include a more in-depth analysis of different plant varieties to broaden the applicability of the findings. Additionally, exploring methods to enhance the leaf wettability in greenhouse environments by regulating the temperature, humidity, and light intensity could yield valuable insights. This would provide new perspectives and opportunities for improving the pesticide application effectiveness and further advancing the research in this field.

Author Contributions: Conceptualization, X.Z. and S.S.; investigation, X.Z. and B.X.; validation, X.Z., B.X., and Q.D.; data curation and writing—original draft, X.Z.; supervision, D.S.; resources, D.S., X.X., and S.S.; funding acquisition, X.X. and S.S.; project administration and writing—review and editing, S.S. All authors have read and agreed to the published version of the manuscript.

Funding: This research was funded by the National Natural Science Foundation of China (32472020, 31671591), Key-Area Research and Development Program of Guangdong Province (2023B0202090001), and China Agriculture Research System of MOF and MARA (CARS-26).

Data Availability Statement: Data are contained within the article.

Conflicts of Interest: The authors declare no conflicts of interest.

References

- Gao, Y.; Guo, R.; Fan, R.; Liu, Z.; Kong, W.; Zhang, P.; Du, F.P. Wettability of pear leaves from three regions characterized at different stages after flowering using the ovrk method. *Pest Manag. Sci.* **2018**, *74*, 1804–1809.
- Delele, M.A.; Nuyttens, D.; Duga, A.T.; Ambaw, A.; Lebeau, F.; Nicolai, B.M.; Verboven, P. Predicting the dynamic impact behaviour of spray droplets on flat plant surfaces. *Soft Matter* **2016**, *12*, 7195–7211.
- He, Y.; Wu, J.; Xiao, S.; Fang, H.; Zheng, Q. Investigating the wettability of rapeseed leaves. *Appl. Eng. Agric.* **2021**, *37*, 399–409.
- Nairn, J.J.; Forster, W.A. Methods for evaluating leaf surface free energy and polarity having accounted for surface roughness. *Pest Manag. Sci.* **2017**, *73*, 1854–1865.
- Wang, H.; Shi, H.; Li, Y.; Wang, Y. The effects of leaf roughness, surface free energy and work of adhesion on leaf water drop adhesion. *PLoS ONE* **2014**, *9*, e107062.
- Nairn, J.J.; Forster, W.A.; van Leeuwen, R.M. Quantification of physical (roughness) and chemical (dielectric constant) leaf surface properties relevant to wettability and adhesion. *Pest Manag. Sci.* **2011**, *67*, 1562–1570.
- Feng, Y.; Guo, X.; Li, Y.; Li, G.; Yu, Q.; Zhang, R. Effects of surface free energy of crops leaves and spray adjuvants on the wettability of pesticide solution on five crop leaves. *Nongyaxue Xuebao* **2022**, *24*, 1466–1472.
- Kang, H.; Graybill, P.M.; Fleetwood, S.; Boreyko, J.B.; Jung, S. Seasonal changes in morphology govern wettability of katsura leaves. *PLoS ONE* **2018**, *13*, e202900.
- Jiang, Y.; Duan, J.; Jiang, T.; Yang, Z. Microscale mechanism of microstructure, micromorphology and janus wettability of the banana leaf surface. *Micron* **2021**, *146*, 103073.
- Leca, A.; Rouby, F.; Saudreau, M.; Lacointe, A. Apple leaf wettability variability as a function of genotype and apple scab susceptibility. *Sci. Hortic.* **2020**, *260*, 108890.
- Papierowska, E.; Szatyłowicz, J.; Samborski, S.; Szewińska, J.; Różańska, E. The leaf wettability of various potato cultivars. *Plants* **2020**, *9*, 504.
- Zhao, X.; Gao, Y.; Zhang, C.; Zhu, Y.; Lei, J.; Ma, Y.; Du, F.; Wettability of ionic surfactants sds and dtab on wheat (*Triticum aestivum*) leaf surfaces. *J. Disper. Sci. Technol.* **2018**, *39*, 1820–1828.
- Zhu, F.; Cao, C.; Cao, L.; Li, F.; Du, F.; Huang, Q. Wetting behavior and maximum retention of aqueous surfactant solutions on tea leaves. *Molecules* **2019**, *24*, 2094.

14. Song, Y.; Huang, Q.; Huang, G.; Liu, M.; Cao, L.; Li, F.; Zhao, P.; Cao, C. The Effects of Adjuvants on the Wetting and Deposition of Insecticide Solutions on Hydrophobic Wheat Leaves. *Agronomy* **2022**, *12*, 2148.
15. Holloway, P.J. Surface factors affecting the wetting of leaves. *Pestic. Sci.* **1970**, *1*, 156–163.
16. Bao, L.; Fan, H.; Chen, Y.; Yan, J.; Yang, T.; Guo, Y. Effect of surface free energy and wettability on the adhesion property of waterborne polyurethane adhesive. *RSC Adv.* **2016**, *6*, 99346–99352.
17. Yuan, Y.; Lee, T.R. *Surface Science Techniques*; Bracco, G., Holst, B., Eds.; Springer: Berlin/Heidelberg, Germany, 2013; pp. 3–34.
18. Guo, H.L.; Xie, Z.; Shaw, J.; Dixon, K.; Jiang, Z.T.; Yin, C.Y.; Liu, X. Elucidating the surface geometric design of hydrophobic australian eucalyptus leaves: Experimental and modeling studies. *Heliyon* **2019**, *5*, e1316.
19. Bachurová, M.; Wiener, J. Free Energy Balance of Polyamide, Polyester and Polypropylene Surfaces. *J. Eng. Fibers Fabr.* **2012**, *7*, 155892501200700411.
20. Lin, H.; Zhou, H.; Xu, L.; Zhu, H.; Huang, H. Effect of surfactant concentration on the spreading properties of pesticide droplets on eucalyptus leaves. *Biosyst. Eng.* **2016**, *143*, 42–49.
21. He, B.; Patankar, N.A.; Lee, J. Multiple equilibrium droplet shapes and design criterion for rough hydrophobic surfaces. *Langmuir* **2003**, *19*, 4999–5003.
22. Fernandez, V.; Khayet, M. Evaluation of the surface free energy of plant surfaces: Toward standardizing the procedure. *Front. Plant Sci.* **2015**, *6*, 510.
23. He, L.; Ding, L.; Waterhouse, G.; Li, B.; Liu, F.; Li, P. Performance matching between the surface structure of cucumber powdery mildew in different growth stages and the properties of surfactant solution. *Pest Manag. Sci.* **2021**, *77*, 3538–3546.
24. Gao, P.; Xie, J.; Yang, M.; Zhou, P.; Liang, G.; Chen, Y.; Sun, D.; Han, X.; Wang, W. Predicting the photosynthetic rate of chinese brassica using deep learning methods. *Agronomy* **2021**, *11*, 2145.
25. Fan, R.; Zhang, X.; Zhou, L.; Cao, C.; Du, F. Research on the wettability of peach leaf surfaces by OWRK method. *Chin. J. Pestic. Sci.* **2011**, *13*, 79–83.
26. Young, T. An essay on the cohesion of fluids. *Philos. Trans. R. Soc. Lond.* **1805**, *95*, 65–87.
27. Wenzel, R.N. Resistance of solid surfaces to wetting by water. *Ind. Eng. Chem.* **1936**, *28*, 988–994.
28. Cassie, A.B.D. Contact angles. *Discuss. Faraday Soc.* **1948**, *3*, 11–16.
29. Cassie, A.B.D.; Baxter, S.; Wettability of porous surfaces. *Trans. Faraday Soc.* **1944**, *40*, 546–551.
30. Zhang, C.; Zhao, X.; Lei, J.; Ma, Y.; Du, F. Wettability of Triton X-100 on Wheat (*Triticum aestivum*) Leaf Surfaces with Respect to Developmental Changes. *Wuli Huaxue Xuebao* **2017**, *33*, 1846–1854.
31. Prajapati, D.G.; Rowthu, S. Unravelling the anisotropic wetting properties of banana leaves with water and human urine. *Surf. Interfaces* **2022**, *29*, 101742.
32. Shao, F.; Wang, L.; Sun, F.; Li, G.; Yu, L.; Wang, Y.; Zeng, X.; Yan, H.; Dong, L.; Bao, Z. Study on different particulate matter retention capacities of the leaf surfaces of eight common garden plants in hangzhou, china. *Sci. Total Environ.* **2019**, *652*, 939–951.
33. Wang, J.; Wu, Y.; Cao, Y.; Li, G.; Liao, Y. Influence of surface roughness on contact angle hysteresis and spreading work. *Colloid Polym. Sci.* **2020**, *298*, 1107–1112.
34. Liu, Y.; Dong, H.; Hu, J.; Zhao, M.; Liu, S.; Zeng, S. Surface free energies and their fractions of different tobacco leaves in Yunnan. *J. Northwest AF Univ.* **2013**, *41*, 75–78.

Disclaimer/Publisher's Note: The statements, opinions and data contained in all publications are solely those of the individual author(s) and contributor(s) and not of MDPI and/or the editor(s). MDPI and/or the editor(s) disclaim responsibility for any injury to people or property resulting from any ideas, methods, instructions or products referred to in the content.